Behavior of Laminated Timber Portal Frames Reinforced with Fiber-reinforced Plastic Laminates under Cyclic Lateral Load

Yo-Jin Song,[a] Seong-Yeob Baek,[b] Hyun-Woo Kim,[b] and Soon-Il Hong [b,*]

This study aimed to enhance the structural performance of a drift joint with a slotted-in steel plate using laminated timber made from small- to medium-diameter timbers. An analysis was conducted to compare and evaluate the structural performance and seismic behavior of laminated timber portal frames reinforced with fiber-reinforced plastic (FRP) laminates, such as glass fiber cloth (GFC), glass fiber reinforced plastic sheet (GS), and carbon-reinforced plastic sheet (CS), under low amplitude cyclic lateral loads, in comparison to unreinforced portal frames (UR). The reinforced portal frame, strengthened by FRP laminates, exhibited higher resistance to strength and stiffness strength degradation due to cyclic loading-induced degradation at low drift angles compared to the unreinforced frame affected by heterogeneous timber. The reinforced portal frame, particularly the GFC and GS, exhibited energy dissipation rates 32% and 17% higher than UR, respectively, making them the most effective in vibration damping. FRP laminates mitigated fiber direction cleavage from drift pin holes. The average maximum moment and average yield moment of the reinforced portal frame increased by 18% and 21%, respectively, due to the alleviation of joint failure. Finally, CS significantly affected the maximum moment, while GFC significantly influenced the yield moment.

DOI: 10.15376/biores.19.4.8739-8757

Keywords: Laminated timber; Portal frame; Joint; Lateral load; Cyclic test; Reinforcement; FRP

*Contact information: a: Institute of Forest Science, Kangwon National University, Chun-Cheon 200-701 Republic of Korea; b: Department of Forest Biomaterials Engineering, Kangwon National University, Chun-Cheon 200-701 Republic of Korea; *Corresponding author: hongsi@kangwon.ac.kr*

INTRODUCTION

When producing structural materials from small- to medium-diameter timber, the processing becomes simpler and more cost-effective than using panels such as glued laminated timber (glulam) or cross-laminated timber (CLT), as the yield of lumber is higher. However, small- to medium-diameter timber may have several defects, such as juvenile wood and knots, significantly reducing its strength and making it disadvantageous for individual use. Laminated timber, which involves gluing many layers of timber, enables the production of large-diameter timber and addresses the structural flaws seen in small- to medium-diameter timber mentioned earlier. Additionally, it is environmentally friendly, as it requires less adhesive due to its smaller bonding surface. Moreover, it enables high-value-added harvesting of thinned logs. Laminated timber has good durability and adhesive performance through relevant research on development projects (Lee *et al.* 2019). Its potential as a structural component resistant to bending and compression loads has been confirmed (Lee *et al.* 2021; Baek *et al.* 2023).

When wide open spaces and longer spans are required in structural elements, moment-resisting structures, such as portal frames, are often necessary to withstand lateral loads (Chen *et al.* 2018). Modern large-diameter timber construction components are typically connected using metal connectors, particularly through metal dowel joints with slotted steel plates, which provide stability and resistance to moments. Due to the low tensile strength in the fiber perpendicular direction and the low shear strength in the fiber parallel direction, the current design methodology generally ignores the moment resistance capacity and focuses only on transmitting shear force and axial force (He and Liu 2015; Liu and Xiong 2018). Despite this, vertical loads or lateral loads such as seismic loads applied to the beam actually generate moments in these timber column-beam joints. On the other hand, the resistance mechanism against the force exerted on the metal dowel joint with slotted plates can be divided into two types: tensile type, which resists the force applied along the dowel axis, and shear type, which resists the force applied perpendicular to the dowel axis. However, the low tensile strength and shear strength resulting from the fiber direction of the mentioned wood lead to vulnerability due to the wood embedment of the dowel and cause severe destruction of the structure in the direction of end distance, such as cleavage and plug shear (Sawata 2015). These failure modes can cause early failure in ductile structures affected by susceptible forces induced by earthquakes, as they degrade the ductility and energy dissipation capacity. Therefore, enhancing the resistance behavior against lateral loads to ensure the stability of the structure is crucial.

Reinforcing structural elements and joints using fiber reinforced plastic (FRP) has been commonly employed in timber construction (Raftery and Harte 2011; Sena-Cruz *et al.* 2012; Raftery and Whelan 2014; Schober *et al.* 2015; Zhu *et al.* 2017; Grunwald *et al.* 2018; Toumpanaki *et al.* 2022). This reinforcement method can improve the flexural performance of the absence and the mechanical characteristics of the joint, particularly demonstrating excellent ability to suppress splitting caused by the fiber direction of wood (Song *et al.* 2017; Lee *et al.* 2021; Kim *et al.* 2022). Above all, FRP possesses several advantageous characteristics that make it suitable for application in timber engineering structures, such as corrosion resistance, high strength-to-weight ratio, and excellent adhesion to wood. There has been a relative lack of research on joints using FRP in structural engineering. The main focus of research has been placed on the 'glued-in' joints using FRP rods to replace metal dowel joints. Some researchers have proposed reinforcement methods that use slotted steel plates and metal dowels to improve the moment resistance performance of column-beam joints.

Santos *et al*. (2013) studied adhesive reinforcement techniques for metal dowel wood joints. The proposed method of reinforcing the area around the hole with carbon fiber reinforced plastic (CFRP) adhesive was found to be more effective in enhancing joint performance and mitigating brittle failure mode (Santos *et al.* 2013). Kim *et al*. (2013) examined the shear performance of bolt joints in laminated timber, considering the arrangement of reinforced glass fiber cloth (GFC) and the volume ratio of reinforcement. The research findings indicate that when the glass fiber cloth (GFC) was positioned in the inner layer of the laminated timber rather than the outer layer, the reinforcement effect was more pronounced for the 1% volume ratio reinforced laminated timber. Additionally, for the 2% volume ratio reinforced laminated timber, the yield shear strength was improved by 22% compared to the unreinforced joint (Kim *et al.* 2013). Xiong *et al*. (2017) conducted a cyclic load test on a single-story portal frame to investigate the lateral resistance of reinforced glued laminated timber column-beam structures. The results revealed that the reinforcement method of wrapping FRP in the joints could inhibit crack initiation and

improve the strength, stiffness, and energy dissipation capacity, indicating that the method using FRP can be applied in engineering practice (Xiong *et al.* 2017). Yang *et al*. (2020) researched to enhance the load transfer capacity of dowel-type joints by wrapping FRP straps around single-bolt timber joints externally or attaching them at various angles. Consequently, the strength of the joint was increased by 50% compared to the control group joint, depending on the appropriate fiber orientation of the FRP. Additionally, the FRP prevented early splitting of the joint, mitigating the failure of the timber. The authors conducted studies to strengthen the timber column-beam joint by FRP reinforcement. The aim was to replace metal dowels and steel plates by reinforcing the plywood with fiberglass and laminating it at high temperatures, as described in Song *et al.* 2014(a, b). Additionally, the structural usability of the laminated beam-column joint was evaluated by inserting the laminate into the joint slot and bonding it, as assessed by Jung *et al.* 2016(a, b). Previous studies imply that the optimal method for enhancing the performance and constructability of a metal dowel joint is to attach FRP laminates with fiber orientation orthogonal to the joint on the outer side of the joint. If a wooden panel is attached to the outer surface of this FRP laminate, it would be possible to improve the aesthetics lacking in previous studies by attaching or covering the FRP on the outer side of the joint.

This paper investigated the behavior of a laminated timber portal frame reinforced with FRP laminates and a slotted-in steel plate drift joint under cyclic lateral loads of low frequencies. The FRP laminates were produced in three types: GFC in fabric form, GFRP sheet in plastic form, and CFRP sheet. The performance enhancement of laminated timber portal frame joints using these laminates was compared to portal frames without reinforcement. The hysteresis loop was used to evaluate the rotational stiffness, moment resistance capacity of the joint, and its seismic behavior under cyclic load. Additionally, the maximum capacity and ductility of the structure, including the failure mode, were assessed by the monotonic load to failure after the cyclic load.

EXPERIMENTAL

Material Properties

Laminated timber

Lumber refers to the dried timber obtained from larch (*Larix kaempferi* (Lamb.) Carr.) with a medium diameter, including the pith. The cross-sectional dimensions of the lumber were 120 mm (height) × 90 mm (width). The average air-dry moisture content of the lumber was 15.0 ± 0.9%, and the average air-dry specific gravity was 0.52 ± 0.03. The laminated timber comprised four lumber pieces with an elastic modulus of 10 GPa. The timber was pressed with a pressure of 1.0 MPa after being coated with a phenol-resorcinol formaldehyde adhesive at a level of 400g/m^2 (single spread) in both flatwise and edgewise orientations (Lee *et al.* 2019). The laminated timber, which was successfully produced, was ultimately processed into a cross-sectional size of 220 mm (height) × 170 mm (width) and used for fabricating portal frames.

FRP laminates

FRP laminates were created by attaching FRP reinforcements to lumber boards to strengthen the portal frame joint made of laminated timber. FRP laminates were manufactured in three different types: glass fiber cloth (GFC) woven with fiberglass filaments crossing each other at right angles, glass fiber reinforced plastic (GFRP) sheets pultruded with resin and longitudinally oriented fibers, and carbon fiber reinforced plastic

(CFRP) sheets (Fig. 1). The reinforcement materials were stacked with a reinforcement ratio of 6.7% (thickness: 6 mm) based on the cross-section of the joint in the portal frame. Kim and Hong (2015) evaluated the fracture toughness of fiberglass laminated timber and reported that when the crack propagation direction of the wood aligns with the fiber array direction of the reinforcement, the fracture toughness of the laminated timber is significantly reduced. According to previous research findings, it has been observed that the two reinforcing materials, excluding the fabric-type GFC, can easily split along the fiber direction of the reinforcement due to embedment by dowels at the joint. To prevent this, GFRP and CFRP were laminated with their fiber orientations perpendicular to each other. The reinforcing materials were manufactured by applying epoxy adhesive and hot pressing them at a temperature of 60 ℃ and a pressure of 1.0 MPa. After curing, they were bonded to a lumber board with a thickness of 18 mm using Polyurethane (PUR) adhesive (P84, Otto-Chemie, Bavaria, Germany). The final dimensions of the FRP laminates were 24 mm × 220 mm × 240 mm (Fig. 2).

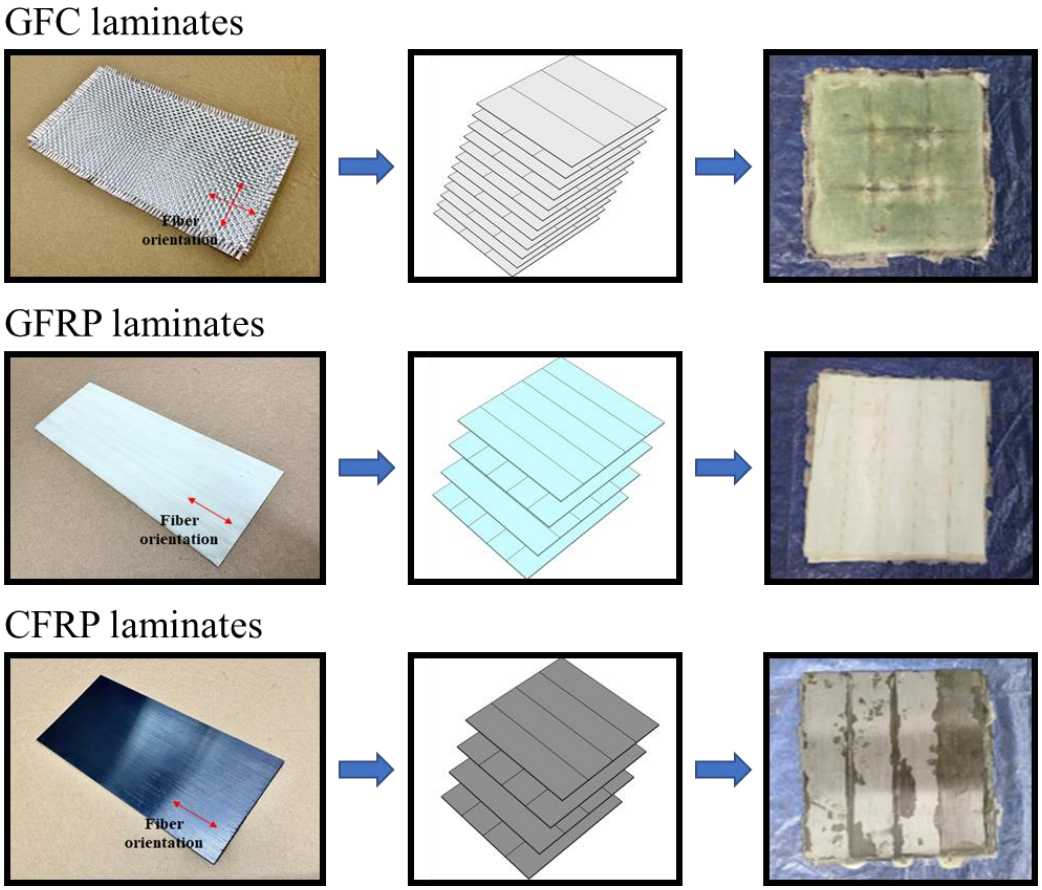

Fig. 1. The manufacturing process of FRP laminates

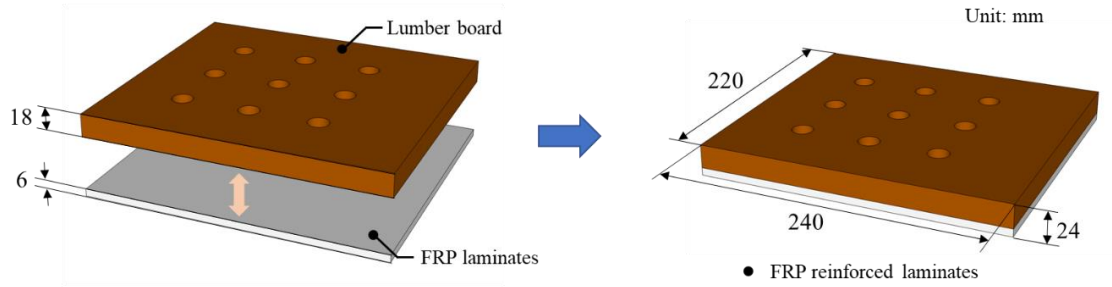

Fig. 2. FRP laminates bonded with lumber board

Test Methods

Fabrication of laminated timber portal frames

The portal frame was constructed with a single span on the ground floor, with a height of 1690 mm from the floor to the center of the beam and a distance of 1930 mm between the centers of the columns (total height: 1800 mm, total width: 2370 mm). The joints of the portal frame were fixed using an inserted drift pin method, as shown in Fig. 3 (a and c). Slots with a thickness of 10 mm and a depth of 240 mm were machined on the column and beam joints. One rolled steel plate, according to KS D 3503 standards (2018), with a thickness of 8 mm, a width of 220 mm, and a length of 440 mm was inserted. The plate was then attached to the beam and column using 16 drift pins with a diameter of 16 mm and a length of 170 mm. The hole positions of the drift pin were designed to have an end distance, edge distance, and spacing, all measuring 3.5 times the diameter of the drift pin (Fig. 3 (b and d)). In the case of the reinforced portal frame, the columns and beams of the joints were partially reinforced with FRP laminates on the outer side, with a depth of 24 mm, width of 220 mm, and length of 240 mm each (Fig. 3 (c and d)). The wooden part of the FRP laminates was attached to the outside side of the FRP surface by applying PUR adhesive. Four types of portal frames were produced, with two frames per type: unreinforced portal frame (UR), portal frame reinforced with GFC laminate (GFC), portal frame reinforced with GFRP laminates (GS), and portal frame reinforced with CFRP laminates (CS) (Table 1).

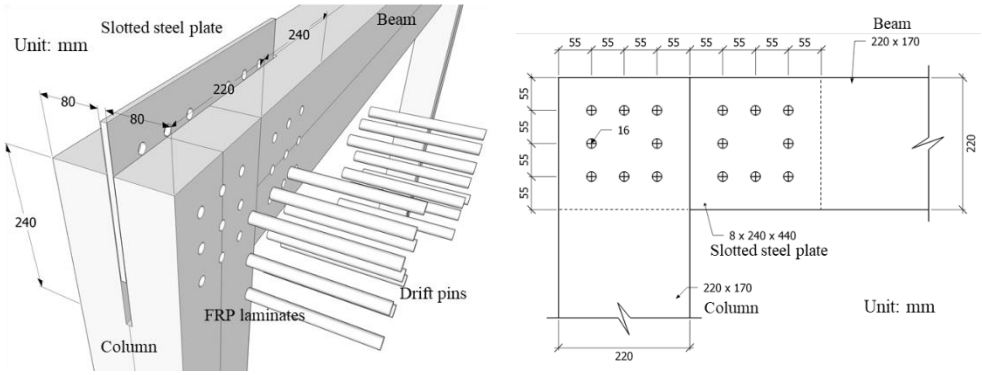

(a) **(b)**

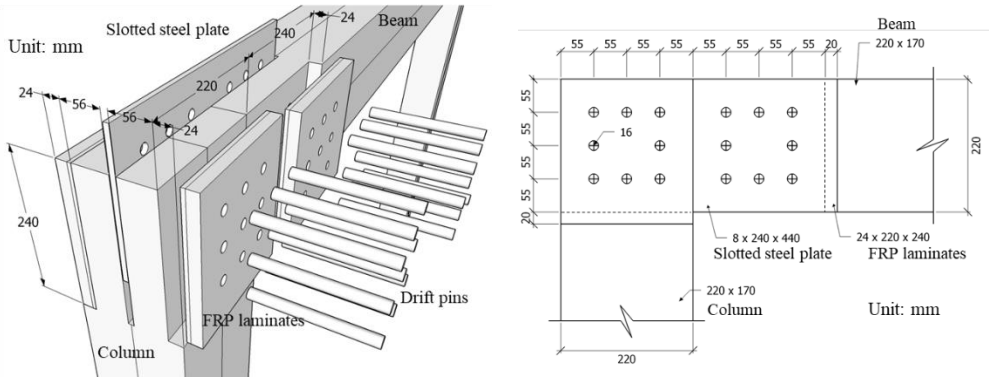

(c) **(d)**

Fig. 3. Layouts of the laminated timber portal frame. (a), (b) Configuration of the laminated timber portal frame. (c), (d) Configuration of the laminated timber portal frame with FRP laminates.

Table 1. Geometry and Joints of Laminated Timber Portal Frames

Portal frame	Beam-column joint	Reinforcement	Beam and column size (mm)	Column spacing (m)	Height (m)	No.
UR	Drift pin and Slotted-in steel-plate	None	220 × 170	2.37	1.8	2
GFC		GFC laminates	220 × 170	2.37	1.8	2
GS		GFRP laminates	220 × 170	2.37	1.8	2
CS		CFRP laminates	220 × 170	2.37	1.8	2

Test setup and instrumentation

Each portal frame, as indicated in Fig. 4, was fixed to the foundation with two steel angle brackets and four high tensile bolts (diameter: mm) per column. Five displacement sensors were installed to obtain the drift angle of the joint. The holder connected to the hydraulic jack was fixed to the beam to transmit the lateral load to the portal frame. To measure the horizontal displacement of the portal frame, displacement gauges (d_1, d_2,) were symmetrically placed at the same height on both sides of the hydraulic jack's plate slot opposite the joint (Fig. 5). Furthermore, a single column (d_3) was installed at a height of 210 mm from the foundation base. For the measurement of vertical displacement of the portal frame, two columns (d_4, d_5) were installed at the bottom of the foundation, each at a height of 100 mm from the ground.

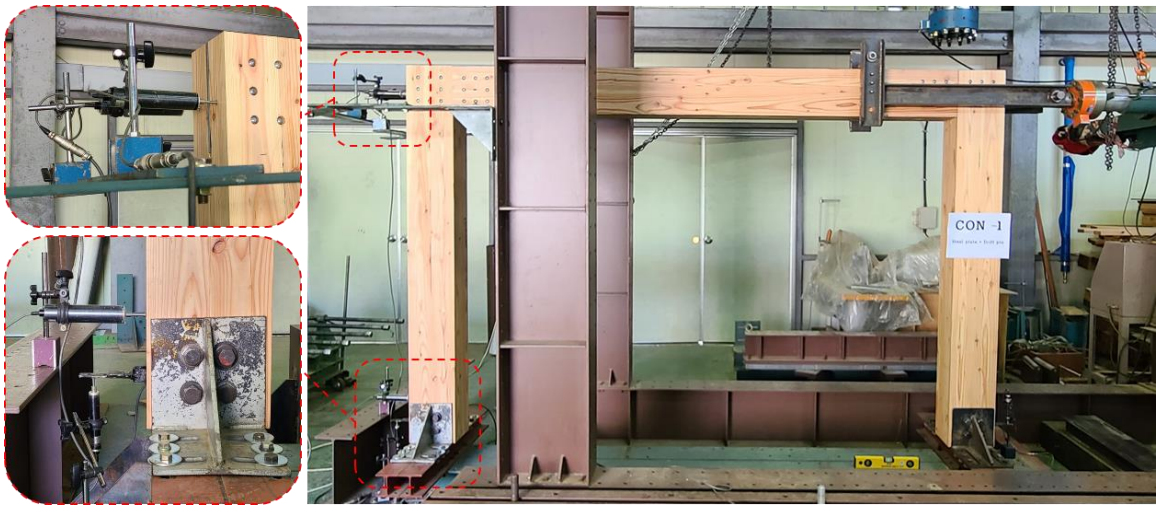

Fig. 4. Test setup for laminated timber portal frames

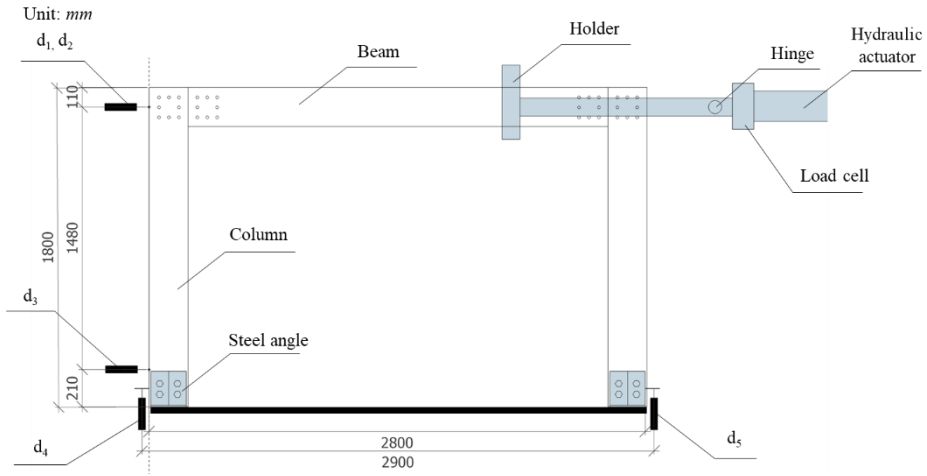

Fig. 5. Test setup and instrumentation for laminated timber portal frame

Loading scheme

The cyclic load tests on the portal frame were conducted using the displacement-centered method. The cyclic load schedule assumes that no vertical load was applied to the structure, according to the Architectural Institute of Japan's (2012) standards. The portal frames were subjected to three cyclic loading cycles in positive and negative directions within each drift angle section (1/450 rad., 1/300 rad., 1/200 rad., 1/150 rad., 1/100 rad., 1/75 rad., 1/50 rad.), as depicted in Fig. 6. The test was terminated if the joint fractured or if the drift angle exceeded 1/15 radians while moving forward. The velocity of the load was 40 mm/min.

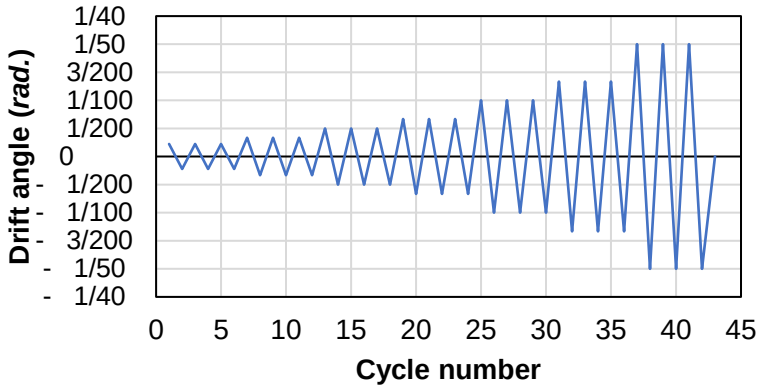

Fig. 6. Cyclic loading protocol

Table 2 presents the horizontal displacement transformation values for the drift angle and the information on the frequency. The joint's effective drift angle (θ) was calculated using the following Eqs. 1, 2, and 3,

$$\theta = \theta_1 - \theta_2 \quad (1)$$

$$\theta_1 = \left(\left(\frac{d_1+d_2}{2}\right) - d_3\right) \div H \quad (2)$$

$$\theta_2 = (d_4 - d_5) \div B \quad (3)$$

where θ represents the effective drift angle of the beam with respect to the plate, θ_1 is the drift angle of the beam with respect to the column, and θ_2 signifies the drift angle of the plate with respect to the column. Furthermore, $d_1, d_2, d_3, d_4,$ and d_5 represent the displacements measured by LVDT 1, LVDT 2, LVDT 3, LVDT 4, and LVDT 5, respectively.

Table 2. Horizontal Displacement According to Drift Angle

Drift angle (*rad.*)	Horizontal displacement (mm)	Cycle number
1/450	3.3	3
1/300	4.9	3
1/200	7.4	3
1/150	9.9	3
1/100	14.8	3
1/75	19.7	3
1/50	29.6	3
1/15 *rad.* or until failure	98.7	Monotonic

RESULTS AND DISCUSSION

Hysteresis Loop

The hysteresis loop serves as a fundamental basis for seismic design, illustrating the relationship between the moment and rotation of portal frame joints under low-cycle loading conditions. The hysteresis loop for each series is graphed in Fig. 7. The moment on the vertical axis represents the total load applied to the timber portal frame joints, which directly cause the stresses generated in the timber portal frame joints. The drift angle on

the horizontal axis is the angle of deformation between the column and beam caused by the moment. The hysteresis loop of the portal frames demonstrated no significant damage during the process, namely in the final drift angle section of 1/50 rad. However, it was observed that the reinforcement in the portal frame joint and the type of FRP laminates used resulted in variations of the slope and magnitude of the hysteresis loop. These differences are speculated to arise from the capacity and stiffness of the joint's load cycle during the first drift angle, as well as the strain hardening of the drift pin and timber during the load cycle, and the strain inhibition performance of FRP laminates based on the reinforcement material. The average maximum moment obtained from the hysteresis loop was 11.6 kN·m, which was the lowest among the portal frames. The GFC laminate, based on the UR, increased the moment of the portal frame by 12%. The moments of GS and CS increased by 22% and 21%, respectively, implying that the laminate manufactured with fabric-type reinforcement had a higher improvement effect on the moment in the cyclic load section than the laminate manufactured with fabric-type reinforcement.

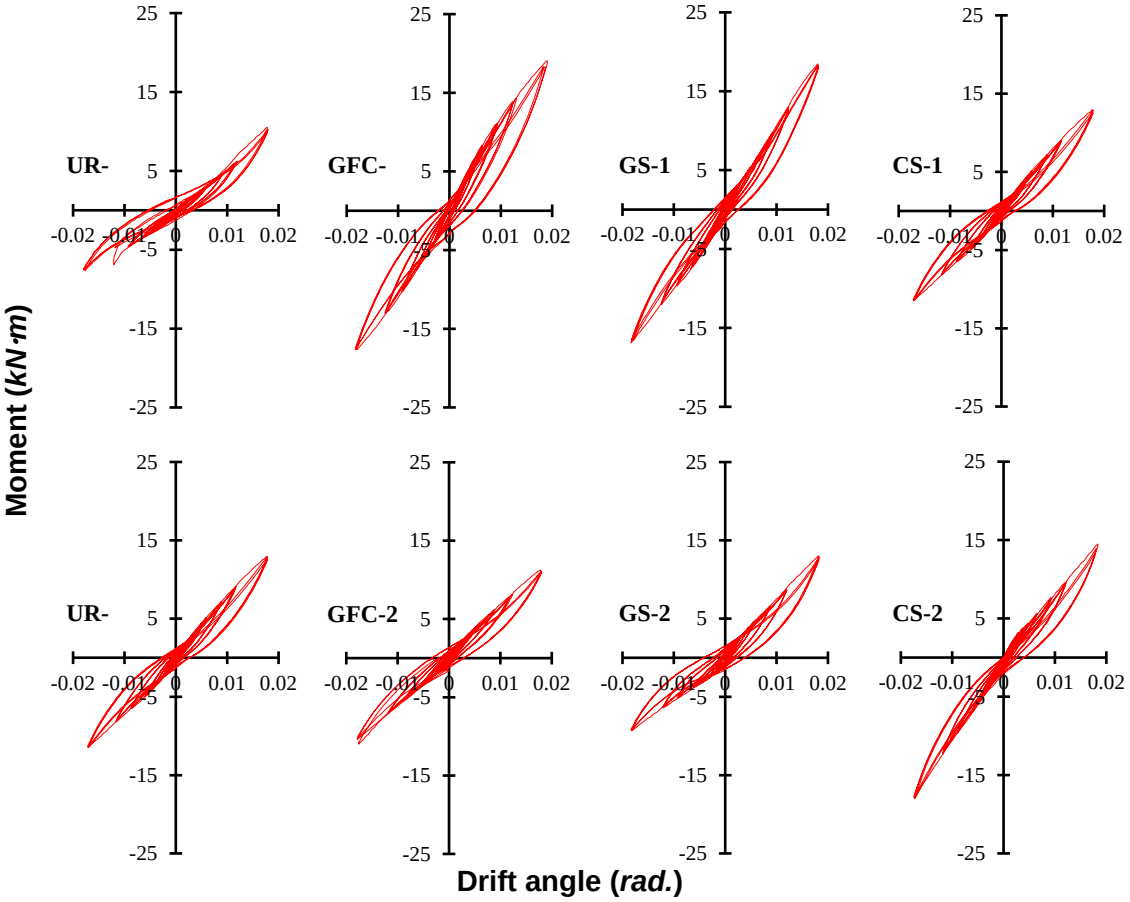

Fig. 7. Hysteresis loops of portal frames

Strength Degradation

The hysteresis loop for cyclic load on structures with joints decreased the load due to the gaps between the joint and the component when compared to the initial load within the same deformation section. The occurrence of defects was determined by the processing form of the joint and the material properties of the joined materials. Particularly, timber structures joined with metal fasteners are susceptible to decreased joint strength between

timber members during cyclic loading. The decrease in intensity is ultimately a crucial indicator of the ability to withstand repetitive seismic movements (Pozza *et al.* 2014; Sheikhtabaghi 2015). Strength degradation (ΔF) refers to the decrease in load when a constant displacement is applied. The value of ΔF was derived from the difference between the maximum load (F_1) at the first-order force and the maximum load (F_3) at the third-order force within the same positive deformation section based on the hysteresis loop of the portal Rahmen frames in Fig. 7, as described in Eq. 4.

$$\Delta F = 1 - (F_3/F_1) \quad (4)$$

Figure 8 represents the average strength degradation of portal frames according to the drift angle. No observed correlation was found between the increase in drift angle and the degradation of strength in the case of UR. The strength degradation of the unreinforced portal frame did not exhibit a specific trend and occurs randomly in all drift angle sections. The highest strength degradation of 4.8% was observed in the last drift angle section (1/50 rad.). However, portal frames reinforced with FRP laminates generally did not exhibit strength degradation in the initial drift angle section. However, as the drift angle increased, there was a gradual increase in strength degradation. In particular, GS and CS improved their strength degradation in the low drift angle section.

In the low drift angle section, UR decreased its strength by nearly 4%. However, across the entire drift angle section, there was a non-directional decrease in strength influenced by the hysteresis phenomenon of the joint due to the heterogeneity of the timber part. In contrast, the reinforced portal frames did not decrease in strength in the initial drift angle section but gradually decreased in strength as the drift angle increased. The decrease in their strength did not exceed 2%, and, unlike UR, the phenomenon of joint history was controlled by FRP-reinforced laminate, resulting in minimal variation in strength degradation.

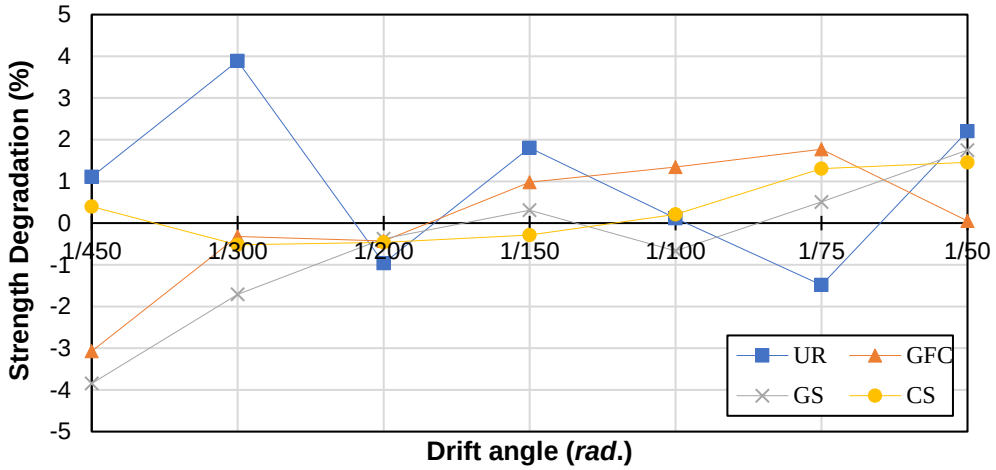

Fig. 8. Average strength degradation at each drift angle

Skeleton Curve

Figure 9 depicts the portal frame's skeleton curve, which is an envelope curve obtained by connecting the peak points of each first cycle of the hysteresis loop in Fig. 7. The stiffness of the portal frame joint recovered from the previous drift angle stage may be determined by using the skeleton curve, and the tendency of the developed curve can be used to assess the potential for early failure of the structural system.

The portal frames were within the elastic range for the applied lateral load, ranging from 1/450 rad. to 1/75 rad. in the cyclic load section. The reinforcement of portal frame joints by FRP laminates impacted the initial stiffness. The reinforced portal frame exhibited a relatively higher stiffness than the unreinforced portal frame in the first drift angle section. The initial stiffness enhancement of the portal frame under cyclic loading allowed for the continuous maintenance of joint stiffness even with increased deformation, which was observed in dead load and live load conditions. The reinforced portal frame, which is reinforced with fabric-type FRP, slightly decreased its stiffness in the 1/50 rad section for positive and negative loads. Moreover, it was observed that its stiffness recovery is slightly lower than other FRP laminates in a larger drift angle section.

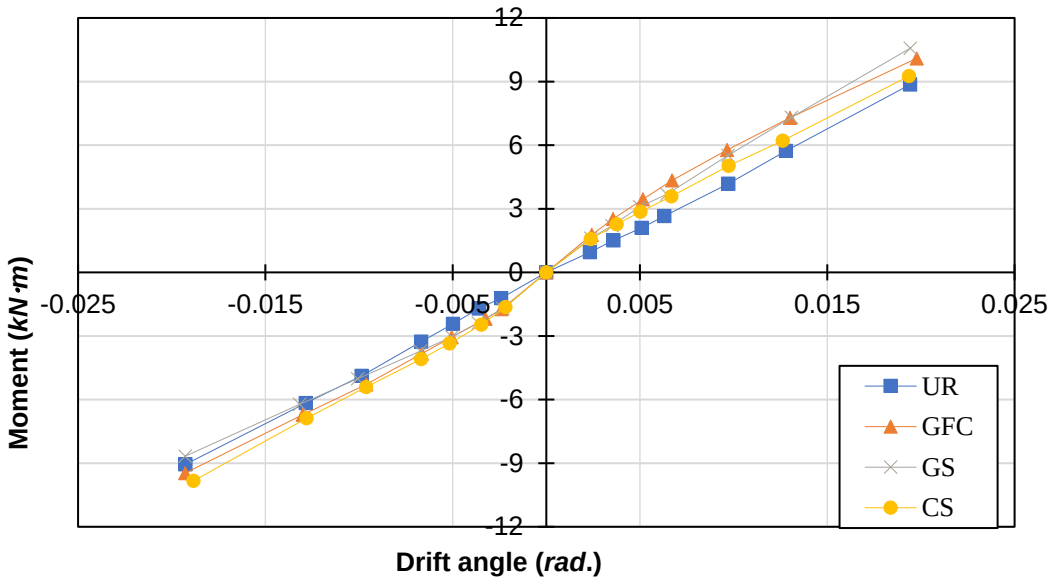

Fig. 9. Average strength degradation at each drift angle (UR: Unreinforced, GFC: Glass fiber cloth, GS: Glass fiber reinforced plastic sheet, CS: Carbon fiber reinforced plastic sheet)

Maximum Load and Failure Mode

Failure mode

The maximum moment of the portal frame was determined by positive loading after applying a cyclic load from 1/450 rad. to 1/50 rad. until the drift angle reached 1/15 rad. or the specimen failed. The yield strength was determined using Yasumura's proposed method, and the stiffness (K) was defined as the slope of the secant line at 10% and 40% of the maximum load (Yasumura1998). The ductility (μ) of the joint was determined by the ratio of the maximum strain (Δ_{max}) to the yield strain (Δ_{yield}). The average maximum moment (M_{max}) of the UR was recorded at 42.5 kN·m, making it the lowest resistance among the portal frames. The portal frames experienced premature failure due to longitudinal shear stress in the timber, originating from the drift pin holes on the outer column or beam, just before reaching the maximum moment during the last monotonic test after cyclic loading. The uncontrolled premature failure acted as a cause for the low measured yield strength (M_{yield}) of the UR. The portal frame exhibited significant fiber direction cleavage from the drift pin holes of all columns and beams, with embedded deformation observed in the outer drift pin holes of the joints (Fig.10). This is a typical failure mode of a wooden structure joint that utilizes a metal dowel. Most drift pins observed after disassembly remained in a straight line without any significant bending deformation.

The reinforced portal frames GFC, GS, and CS showed an average maximum moment increase of 12%, 16%, and 27%, respectively, compared to UR. The average yield moment increased by 38%, 16%, and 10% for GFC, GS, and CS, respectively. The reinforced portal frames did not experience premature failure, unlike UR. Instead, they failed at the maximum moment or after reaching the maximum moment (Fig. 11, Fig. 12, Fig. 13). However, similar to UR, the splitting caused by longitudinal shear stress in the wood still determined the maximum moment. Failure was not observed in the FRP-reinforced laminate on the outer side of the joint, but splitting occurred in the inner wooden part of the joint, similar to UR. An important observation is that plastic hinges were observed in more drift pins than in UR, indicating a higher likelihood of more damage to the wood caused by the drift pins. However, the splitting of timber was significantly reduced in the joints of reinforced portal frames compared to that of unreinforced frames. This confirmed the effectiveness of FRP laminate reinforcement in improving failure mode.

Although no significant difference in the occurrence of cleavage was seen depending on the kind of FRP laminates, the FRP properties caused variations in the deformation of drift pins. Specifically, a greater degree of deflection in the drift spindles of the CS was observed (Fig. 13), implying that the mechanical performance of CFRP laminates was superior to that of GFC or GFRP, and it may be considered the factor that had the most influence on the increase of the maximum moment in a portal frame.

Table 3. Structural Characteristics of Portal Frames with Cyclic Lateral Loads

Specimens	M_{max} (kN)	Δ_{max} (mm)	M_{yield} (kN)	Δ_{yield} (mm)	K (kN/mm)	μ
UR-1	38.70	114.52	19.41	49.73	0.31	2.30
UR-2	46.33	120.35	28.95	55.18	0.39	2.18
GFC-1	50.44	114.39	36.72	73.77	0.40	1.55
GFC-2	44.38	115.92	29.99	71.28	0.31	1.63
GS-1	45.22	119.97	32.17	61.39	0.42	1.95
GS-2	53.03	109.71	23.96	49.82	0.37	2.20
CS-1	47.78	110.49	22.80	45.24	0.36	2.44
CS-2	60.31	135.75	30.43	64.55	0.37	2.10

Fig. 10. Failure modes of laminated timber frame UR

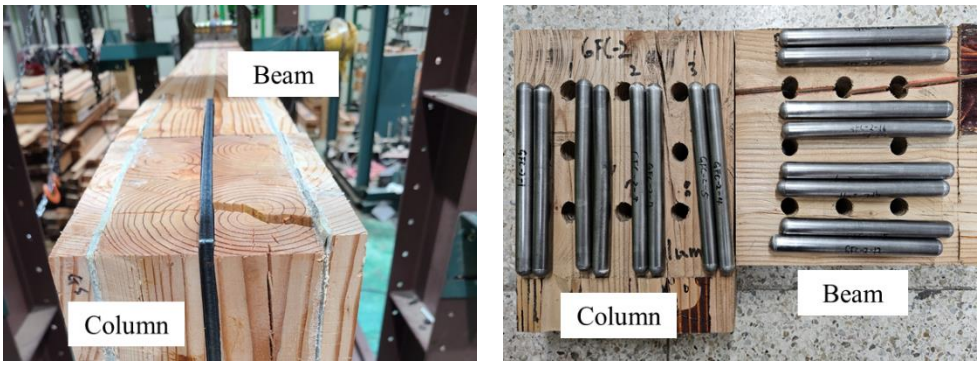

Fig. 11. Failure modes of laminated timber frame GFC

The drift pins of the reinforced portal frame experienced minimal flexural distortion; however, embedded deformation occurred quite significantly in the internal drift pin holes of the laminate. These failure modes were caused by an increase in yield moment (M_{yield}) and yield strain (Δ_{yield}), and the increase in both strength properties ultimately resulted in decreased ductility. Unlike the skeleton curve for the hysteresis loop, the little difference in stiffness between portal frames in the final yield stage indicates that FRP laminates had a greater impact on cyclic load than monotonic load.

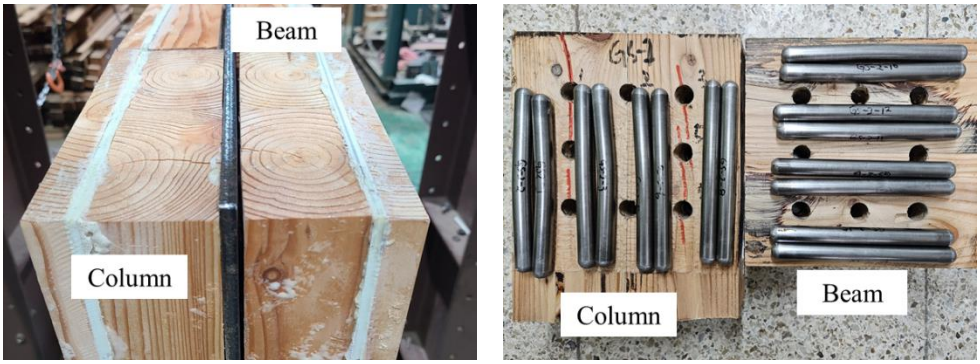

Fig. 12. Failure modes of laminated timber frame GS

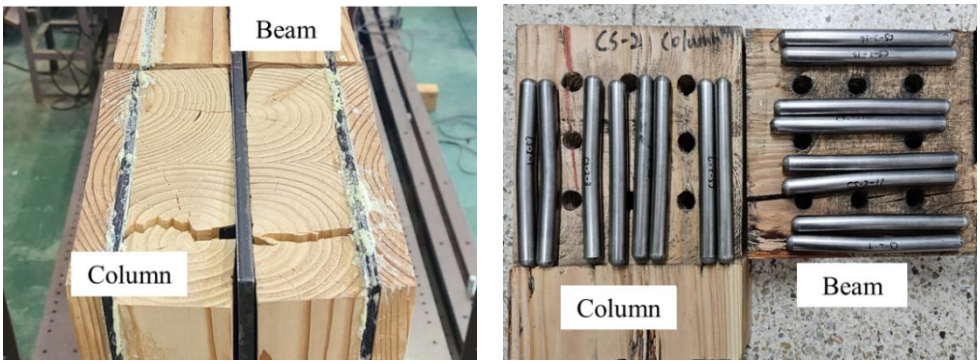

Fig. 13. Failure modes of laminated timber frame CS

Cumulative Energy Dissipation

The seismic performance of wooden structural elements can be comprehensively discussed based on their cumulative energy dissipation capacity (E_d) and equivalent viscous damping ratio (EVD). The energy dissipation capacity is the ability of a portal

frame to absorb seismic energy in each drift angle section, represented by the area enclosed by the load-deformation curve over the same loading cycle, as shown in Fig. 14. This paper calculated the cumulative energy dissipation capacity using the definite integral of the load-deformation curve for the third loading of each load cycle. The energy consumed by the hysteresis characteristics between cyclic load cycles with the equivalent viscous damping ratio was quantified, representing the hysteresis damping properties of the joint at a specific load. The equivalent viscous damping ratio (v_{eq}) was calculated according to Ep. 5 and was represented as the ratio of available potential energy (E_p) to energy dissipation (E_d), as displayed in Fig. 14.

$$v_{eq} = E_d/2\pi E_p \quad (5)$$

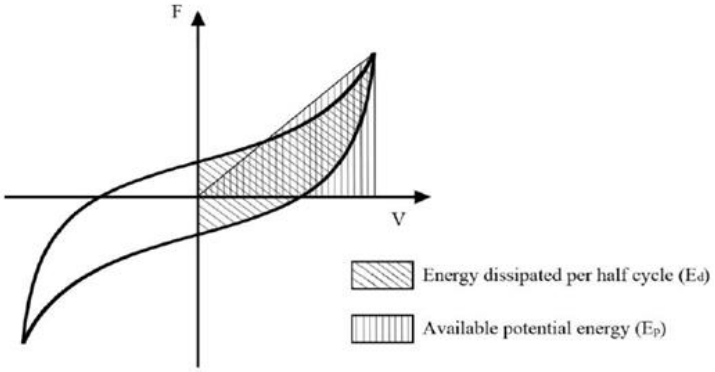

Fig. 14. Dissipation energy and available potential energy definitions (Din 2002)

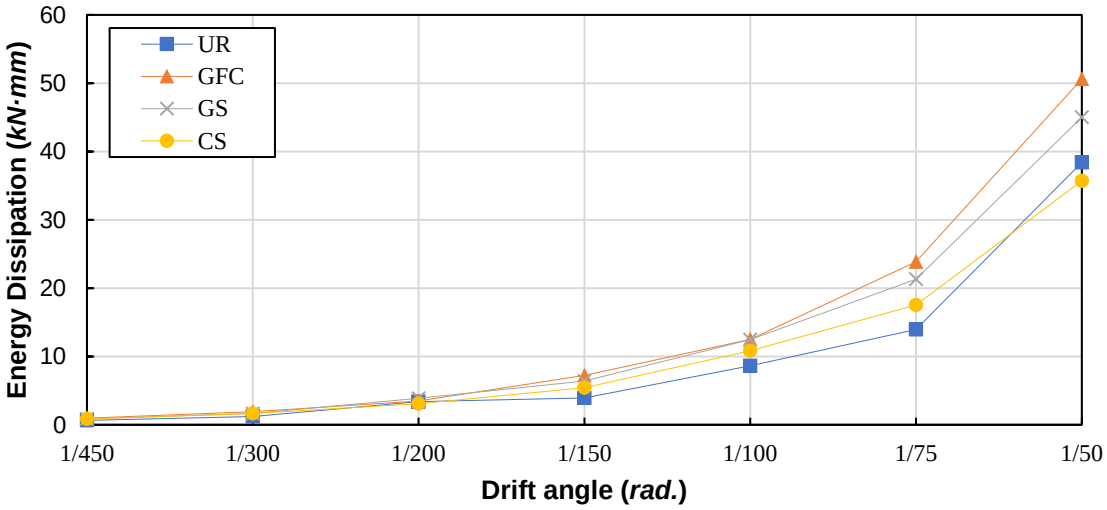

Fig. 15. Cumulative energy dissipation

Figure 15 illustrates the energy dissipation of the portal frame as the drift angle increased. The reinforcement of joints by FRP laminates in the first drift angle section (1/450 to 1/200 rad.) did not impact the increase of energy dissipation in the portal frame. The energy dissipation varied depending on the FRP reinforcement and type, with a noticeable difference starting from 1/150 rad. and becoming more significant from 1/75 rad. The final cumulative energy dissipation increased by 32% and 17% for GFC and GS,

respectively, based on the UR. Despite the superior mechanical properties of CFRP, a reinforcing material that constitutes a reinforced laminate in CS, it was measured to have 7% lower energy dissipation than the UR. This is related to the fact that, as mentioned before about the 'failure mode,' drift pins with plastic hinges were observed most frequently in CS. In contrast, the energy dissipation of GFC, which was laminated with fiberglass in fabric form, was significantly improved; hence, it is claimed that a considerable amount of energy was lost due to the deformation of the reinforced laminate through the pressure of the drift pin, which is a characteristic of the reinforcement's fabric structure.

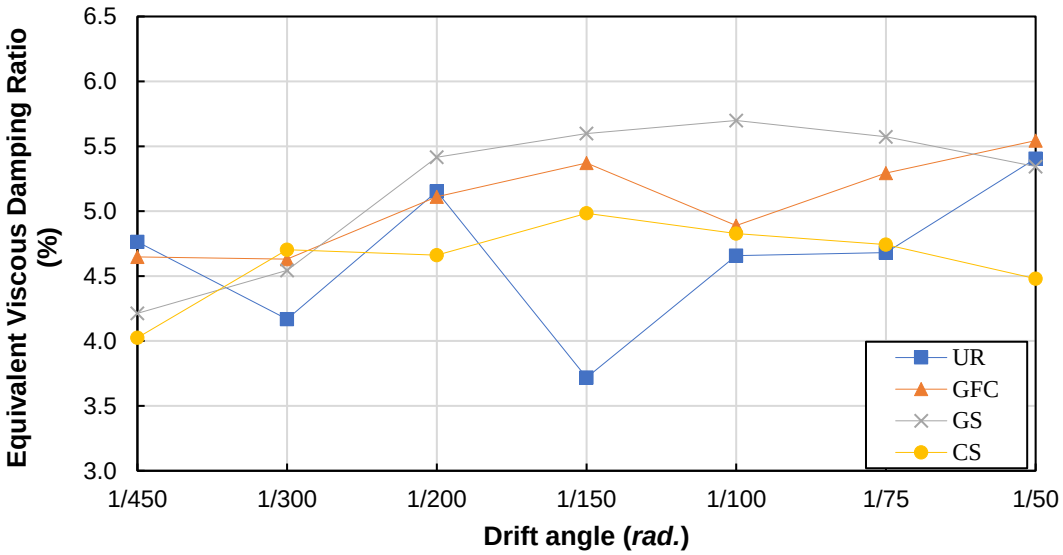

Fig. 16. Equivalent viscous damping ratio (UR:)

Figure 16 represents the average equivalent viscous damping ratio of portal frames' positive and negative loads according to the drift angle. The characteristic values of the equivalent viscous damping ratio were calculated as a percentage. The equivalent viscous damping ratio of the portal frames was measured to be low at initial drift angles of 1/450 rad and 1/300 rad. due to the continued looseness of the gap between the drift pin inserted into the joint and the wood. When considering the joint's potential energy, the average equivalent viscous damping ratio of the unreinforced portal frame, UR, was measured to be 4.6%, which is the lowest among the portal frames. However, the standard deviation (S.D) was 1.7%, indicating a significant variation in the equivalent viscous damping ratio. Among the reinforced portal frames, the equivalent viscous damping ratio of the CS showed no significant difference compared to the UR, with a value of 4.6%. However, the standard deviation (SD) decreased to 0.9%, reducing the variability of the equivalent viscous damping ratio. The corresponding viscous damping ratios of GFC and GS were measured to be 5.1% and 5.2%, respectively, which were higher than the remaining two portal frames. The standard deviation (SD) for the equivalent viscous damping ratio of the GFC is particularly low at 0.6% (compared to 1.2% for GS), indicating that this reinforcement system's vibration damping of the portal frame is the most effective.

CONCLUSIONS

The present study evaluated the behavior of a laminated timber portal frame reinforced with fiber-reinforced plastic (FRP) laminates and featuring a drift joint with a slotted-in steel plate under cyclic lateral load. The hysteresis loop of a portal frame under cyclic load was used to determine the joints' load-carrying capacity, stiffness, energy dissipation, and equivalent viscous damping ratio. After the cyclic load schedule, the portal frames' maximum strength, yield strength, and ductility were obtained using monotonic loading.

1. The reinforcement provided by FRP laminates generated more plastic hinges in the drift pin compared to the unreinforced portal frame. However, it mitigated the fiber direction cleavage in the joint. Furthermore, unlike unreinforced portal frames that experienced localized failure in low-deformation sections, reinforced portal frames reach their maximum load or fail after reaching their maximum load. As a result, carbon fiber-reinforced plastic (CFRP) laminates increased the maximum moment by 27%, whereas glass fiber cloth (GFC) laminates increased the yield moment by 38%.
2. Under cyclic lateral load, the strength degradation of unreinforced portal frame joints due to the hysteresis phenomenon was irregularly influenced by the heterogeneity of the timber, resulting in a maximum decrease of up to 4%. On the other hand, reinforcement of joints by FRP laminates was designed to gradually decrease in strength as deformation increases, not exceeding a maximum of 2%. Furthermore, FRP laminates enabled the maintenance of joint stiffness in both positive and negative loading, even under increased deformation.
3. In the small drift angle section, FRP laminates did not create a significant difference in cumulative energy dissipation. However, as the drift angle increased, the energy dissipation capacity differed, depending on the FRP reinforcement and type. The energy dissipation of the portal frame, particularly due to GFC laminate, exhibited the highest increase of 32%. The average equivalent viscous damping ratio was the highest for the GFC laminate and GS laminate. Similarly, the GFC laminate showed the lowest variation in the equivalent viscous damping ratio, confirming that these reinforcement systems are the most effective in dampening portal frames' vibrations. In summary, the joints of unreinforced timber portal frames, which are influenced by lateral forces, are generally vulnerable to fiber direction cleavage caused by metal dowel embedment. External reinforcement of the joint by FRP laminates can help alleviate the fiber direction cleavage of wood and improve resistance to lateral loads.

ACKNOWLEDGEMENTS

This study was conducted as a basic research project supported by the Korea Research Foundation with funding from the Korean Ministry of Education in 2016 (Grant No. R1D1A1B01011163).

Author Contributions

Yo-Jin Song: Methodology, Formal analysis, Writing - Original Draft, Writing - Review & Editing; Seung-Youp Baek: Investigation, Data Curation; Hyun-Woo Kim:

Investigation, Visualization; Soon-Il Hong: Conceptualization, Writing - Review & Editing, Funding acquisition.

Declaration of Competing Interests

The authors declare that they have no known competing financial interests or personal relationships that could have appeared to influence the work reported in this paper.

REFERENCES CITED

AIJ (2015). "Standard for structural design of timber structures," Architectural Institute of Japan, Tokyo.

Baek, S. Y., Song, Y. J., Kim, H. W., and Hong, S. I. (2023). "Bending strength prediction and finite element analysis of larch structural beams," *BioResources* 18(1), 1824-1835. DOI: 10.15376/biores.18.1.1824-1835

Chen, Z., Popovski, M., and Gerber, A. (2018). "Seismic performance of post-tensioned moment-resisting portal frames," in: *15th World Conference on Timber Engineering WCTE2018*, Seoul, Republic of Korea.

DIN (2022). "Timber structures, test methods, cyclic testing of joints made with mechanical fasteners," Beuth Verlag, Berlin, Germany. DOI: 10.3403/02536208

Grunwald, C., Kaufmann, M., Alter, B., Vallée, T., and Tannert, T. (2018). "Numerical investigations and capacity prediction of G-FRP rods glued into timber," *Composite Structures* 202, 47-59. DOI: 10.1016/j.compstruct.2017.10.010

He, M. J., and Liu, H. F. (2015). "Comparison of glulam post-to-beam connections reinforced by two different dowel-type fasteners," *Construction and Building Materials* 99, 99-108. DOI: 10.1016/j.conbuildmat.2015.09.005

Jung, H. J., Song, Y. J., Lee, I. H., and Hong, S. I. (2016a). "Lateral load performance evaluation of larch glulam portal frames using GFRP-reinforced laminated plate and GFRP rod," *Journal of the Korean Wood Science and Technology* 44(1), 30-39. DOI: 10.5658/wood.2016.44.1.30

Jung, H. J., Song, Y. J., Lee, I. H., and Hong, S. I. (2016b). "Moment resistance performance evaluation of larch glulam joints using GFRP-reinforced laminated plate and GFRP rod," *Journal of the Korean Wood Science and Technology* 44(1), 40-47. DOI: 10.5658/wood.2016.44.1.40

Kim, D. H., Yu, S. H., Song, Y. J., Lee, I. H., and Hong, S. I. (2022). "Moment resistance performance of larch laminated timber beam-column joints reinforced with CFRP," *Wood and Fiber Science* 54(1), 14-23. DOI: 10.22382/wfs-2022-02

Kim, K. H., and Hong, S. I. (2015). "Fracture toughness of glass fiber reinforced laminated timbers," *Journal of The Korean Wood Science and Technology* 43(6), 861-867. DOI: 10.5658/wood.2015.43.6.861

Kim, K. H., Song, Y. J., and Hong, S. I. (2013). "Shear strength of reinforced glulam-bolt connection by glass fiber combination," *Journal of the Korean Wood Science and Technology* 41(1), 51-57. DOI: 10.5658/wood.2013.41.1.51

KS D 3503 (2018). "Rolled steels for general structure," Korean Agency for Technology and Standards, Seoul, Korea.

Lee, I. H., Song, Y. J., and Hong, S. I. (2021). "Tensile shear strength of steel plate-reinforced larch timber as affected by further reinforcement of the wood with carbon

fiber reinforced polymer (CFRP)," *BioResources* 16(3), 5106-5117. DOI: 10.15376/biores.16.3.5106-5117

Lee, I. H., Song, Y. J., Song, D. B., and Hong, S. I. (2019). "Results of delamination tests of FRP-and steel-plate reinforced larix composite timber," *Journal of the Korean Wood Science and Technology* 47(5), 655-662. DOI: 10.5658/wood.2019.47.5.655

Liu, Y., and Xiong, H. (2018). "Lateral performance of a semi-rigid timber frame structure: Theoretical analysis and experimental study," *Journal of Wood Science* 64, 591-600. DOI: 10.1007/s10086-018-1727-7

Pozza, L., Scotta, R., Trutalli, D., Pinna, M., Polastri, A., and Bertoni, P. (2014). "Experimental and numerical analyses of new massive wooden shear-wall systems," *Buildings* (4), 355-374. DOI: 10.3390/buildings4030355

Raftery, G. M., and Harte, A. M. (2011). "Low-grade glued laminated timber reinforced with FRP plate," *Composites Part B: Engineering* 42, 724-735. DOI: 10.1016/j.compositesb.2011.01.029

Raftery, G. M., and Whelan, C. (2014). "Low-grade glued laminated timber beams reinforced using improved arrangements of bonded-in GFRP rods," *Construction and Building Materials* 52, 209-220. DOI: 10.1016/j.conbuildmat.2013.11.044

Santos, C. L., de Jesus, A. M., Morais, J. J., and Fontoura, B. F. (2013). "An experimental comparison of strengthening solutions for dowel-type wood connections," *Construction and Building Materials* 46, 114-127. DOI: 10.1016/j.conbuildmat.2013.03.021

Sawata, K. (2015). "Strength of bolted timber joints subjected to lateral force," *Journal of Wood Science* 61, 221-229. DOI: 10.1007/s10086-015-1469-8

Schober, K. U., Harte, A. M., Kliger, R., Jockwer, R., Xu, Q., and Chen, J. F. (2015). "FRP reinforcement of timber structures," *Construction and Building Materials* 97, 106-118. DOI: 10.1016/j.conbuildmat.2015.06.020

Sena-Cruz, J., Branco, J., Jorge, M., Barros, J. A., Silva, C., and Cunha, V. M. (2012). "Bond behavior between glulam and GFRP's by pullout tests," *Composites Part B: Engineering* 43(3), 1045-1055. DOI: 10.1016/j.compositesb.2011.10.022

Sheikhtabaghi, M. S. (2015). *Continuity Connection for Cross Laminated Timber (CLT) Floor Diaphragms*, M.Sc. Thesis University of New Brunswick, Fredericton, Canada.

Song, Y. J., Hong, S. I., Suh, J. S., and Park, S. B. (2017). "Strength performance evaluation of moment resistance for cylindrical-LVL column using GFRP reinforced wooden pin," *Wood Research* 62(3), 417-426.

Song, Y. J., Jung, H. J., Kim, D. G., Kim, S. I., and Hong, S. I. (2014a). "Performance evaluation for bending strength and tensile type shear strength of GFRP Reinforced Laminated wooden pin," *Journal of The Korean Wood Science and Technology* 42(3), 258-265. DOI: 10.5658/wood.2014.42.3.258

Song, Y. J., Jung, H. J., Park, H. H., Lee, H. Y., and Hong, S. I. (2014b). "Evaluation of the moment resistance joint strength of larch glulam using glass fiber reinforced wood plate," *Journal of the Korean Wood Science and Technology* 42(5), 571-578. DOI: 10.5658/wood.2014.42.5.571

Toumpanaki, E., and Ramage, M. (2022). "Cyclic loading of glued-in FRP rods in timber: Experimental and analytical study," *Journal of Composites for Construction* 26(2), article 04021075. DOI: 10.1061/(asce)cc.1943-5614.0001182

Xiong, H., Liu, Y., Yao, Y., and Li, B. (2017). "Experimental study on the lateral resistance of reinforced glued laminated timber post and beam structures," *Journal of Asian Architecture and Building Engineering* 16(2), 379-385. DOI: 10.3130/jaabe.16.379

Yang, J. Q., Smith, S. T., Wu, Y. F., and Feng, P. (2020). "Strengthening single-bolt timber joints with externally bonded CFRP composites," *Structures* 28, 2671-2685. DOI: 10.1016/j.istruc.2020.10.024

Yasumura, M. (1998). "Estimating seismic performance of wood-framed structures," in: *International Wood Engineering Conference*, Lausanne, Switzerland.

Zhu, H., Faghani, P., and Tannert, T. (2017). "Experimental investigations on timber joints with single glued-in FRP rods," *Construction and Building Materials* 140, 167-172. DOI: 10.1016/j.conbuildmat.2017.02.091

Article submitted: July 22, 2024; Peer review completed: August 31, 2024; Revised version received: September 5, 2024; Accepted: September 6, 2024; Published: October 1, 2024.
DOI: 10.15376/biores.19.4.8739-8757